

Remarks on the Proper Use of the Broken Symmetry Approach to Magnetic Coupling

R. Caballol and O. Castell

Departament de Química, Universitat Rovira i Virgili, Pl. Imperial Tàrraco 1, 43005 Tarragona, Spain

F. Illas* and I. de P. R. Moreira

Departament de Química Física, Universitat de Barcelona, C/Martí i Franqués 1, 08028 Barcelona, Spain

J. P. Malrieu

Laboratoire de Physique Quantique, IRSAMC, Université Paul Sabatier 118, route de Narbonne, 31062 Toulouse Cedex, France

Received: April 4, 1997; In Final Form: June 27, 1997[⊗]

The effect of nonorthogonality in the broken symmetry approach to magnetic coupling has been explicitly considered for the first time in Hartree–Fock and a variety of DFT methods. On the basis of the results for three different systems, representative of a variety of physical situations it is shown that the most often quoted trend concerning the much larger degree of delocalization of magnetic orbitals obtained from DFT, as opposed to Hartree–Fock, is not fully justified. A new and simple way to relate the overlap integral entering into the calculation and the spin density is proposed and tested in a variety of model systems.

I. Introduction

The physical description of magnetic coupling in a broad class of chemical compounds including organic biradicals, inorganic complexes, and ionic solids is based on the use of the well-known Heisenberg Hamiltonian,^{1,2} which for two interacting particles with total spin angular momenta S_1 and S_2 may be written as

$$\hat{H} = -J\hat{S}_1\hat{S}_2 \quad (1)$$

J is referred to as the magnetic coupling constant and the convention sign is taken in such way that positive J means ferromagnetic coupling (in order to compare with other works one may caution that some authors use $2J$ instead of J and may or may not use the negative sign). The eigenfunctions of the Heisenberg Hamiltonian are simply spin eigenfunctions, and J is directly related to the energy difference corresponding to these eigenstates.

Attempts to relate the Heisenberg description of magnetic interactions to the electronic structure of a given system have been undertaken by several authors.^{3–6} A particular aspect concerns the use of ab initio techniques of electronic structure to obtain suitable approximations to the spin eigenstates involved in the magnetic interactions and, hence, to be able to explain the experimental value of J . Recently, a number of theoretical studies have shown the power of ab initio techniques to quantitatively describe magnetic interaction in binuclear complexes^{7–14} and also in cluster models of ionic solids.^{15–24} It is important to stress the fact that, in all cases, the successful description of such a delicate physical property lies in the appropriate mapping between the Heisenberg spin eigenstates and the suitable ab initio electronic states.

An alternative approach to the use of spin eigenfunctions has also been proposed by Noodleman et al.^{25–32} This approach makes use of an unrestricted, or spin polarized, formalism and of a broken symmetry solution for the low-spin state. This approach was earlier applied in the framework of $X\alpha$ density

functional theory. Because of the limitations of this primitive density functional formalism, the application of the broken symmetry approach was quite narrow. However, the apparent numerical success of recently proposed exchange correlation functionals prompted different groups to make use of this approach to compute and predict the magnetic coupling constant of different compounds.^{33–37} The mapping of the eigenvalues and eigenstates of the exact nonrelativistic Hamiltonian into a Heisenberg Hamiltonian requires the definition of a model space expressed from localized orthogonal orbitals or the equivalent symmetry-adapted molecular orbitals. This mapping is straightforward for the simplest two electrons in two atomic orbitals problem but requires additional argumentation if more complex cases are considered.^{15–24} In these cases, it is customary to derive the relationship between J and the energy difference of pure spin states using the proper mapping. However, even for the simplest two electrons in two atomic orbitals problem, the correspondence is less evident when spin-unrestricted and nonorthogonal orbitals are used. While this fact has been properly pointed out by Noodleman²⁶ (see also ref 32), it is often ignored or oversimplified. For the sake of simplicity, let us consider the case of a Cu binuclear complex or dimer. From either Heisenberg or exact Hamiltonians it follows that the states involved are a singlet, S, and a triplet, T, and with the definition of the Heisenberg Hamiltonian given by eq 1, the magnetic coupling constant may be written as

$$J = E(S) - E(T) \quad (2)$$

However, in the broken symmetry approach the unrestricted spin states used are the triplet, T', and the broken symmetry solution, BS, and it is easy to show (vide infra) that

$$J = \frac{2(E_{BS} - E_T)}{1 + S_{ab}^2} \quad (3)$$

where S_{ab} is the overlap integral between the magnetic α and β orbitals of the broken symmetry solution. Despite the simplicity of eq 3, it is often oversimplified by taking either $S_{ab} = 0$, strong

[⊗] Abstract published in *Advance ACS Abstracts*, September 15, 1997.

orthogonal or localized limit, or $S_{ab} = 1$, strong delocalized limit. Notice that the value of J computed assuming one or the other limit differs by 100%. Moreover, the choice for a given limit is more based on the proximity of experimental and calculated values than on a rigorous physical or computational basis.^{33–35} Sometimes, DFT-based calculations assume the strong delocalized limit using as the only argument the unproven tendency of DFT to result in magnetic orbitals that are more delocalized than those from unrestricted Hartree–Fock (UHF) calculations.³⁶ Other authors also use DFT formalism to determine the magnetic coupling constant, employing again the broken symmetry approach but assuming the strong localized limit.³⁷ Clearly, both limits cannot hold, and it is necessary to further investigate this point; this is precisely the goal of the present work.

In this paper we use three different models to investigate the effect of nonorthogonality in eq 3 by explicit computation of the overlap integral for different methodologies that go from the UHF to the local density approximation (LDA), passing through some generalized gradient functionals. Our selected examples include the H–He–H model system, often used as a benchmark, the $[\text{Cu}_2\text{Cl}_6]^{2-}$ binuclear complex, and a cluster model representation of the La_2CuO_4 superconductor parent compound. We will show that, for the systems studied, the use of the strong delocalized limit should be avoided. In addition, we will present a simple way to understand the effect of nonorthogonality by showing that a qualitative relationship between the magnitude of the overlap matrix element and the spin density on the magnetic centers exists. If no additional information is available, the use of the strong localized limit is recommended.

II. The Broken Symmetry Approach, the Nonorthogonality Problem, and Its Relationship to Spin Density

To investigate the effect of nonorthogonality on the calculation of the magnetic coupling constant, let us summarize the main points of the broken symmetry approach. We begin by considering again the case of a Cu binuclear complex. As commented above the magnetic coupling constant is related to the energy difference associated to the singlet and triplet electronic states. In the broken symmetry approach one starts by using an unrestricted formalism to compute a triplet state, T' , which can be written as

$$|T'\rangle = |\dots i_A j_B\rangle \quad (4)$$

where “ i_A ” and “ j_B ” stand for the open shell localized α spin orbitals and we use T' to specify that this is the spin polarized, UHF, solution chosen to approach the pure triplet state defined by T in eq 2. If spin contamination, inherent to the use of an unrestricted formalism, is small one can assume that T' is a good approximation to the triplet state. In the following we will accept that T' is a good representation of the high-spin state. Next, a broken symmetry solution, BS, with total $S_z = 0$ is obtained. Notice that two different BS solutions are possible namely

$$\begin{aligned} |BS_1\rangle &= |\dots \bar{a} b\rangle \\ |BS_2\rangle &= |\dots \bar{b} a\rangle \end{aligned} \quad (5)$$

Now, one realizes that the magnetic orbitals entering into the definition of the BS solutions may be expressed as

$$a = \lambda i_A + \mu j_B$$

$$b = \mu i_A + \lambda j_B \quad (6)$$

with $\lambda^2 + \mu^2 = 1$

Using the two BS solutions it is possible to write the symmetry and spin adapted configuration state function for the spin-polarized solution approaching the singlet. As in the case of the triplet, we use S' to differentiate from the pure S singlet.

$$|S'\rangle = \frac{|BS_1\rangle + |BS_2\rangle}{\sqrt{2(1 + \langle BS_1|BS_2\rangle)}} \quad (7)$$

where $\langle BS_1|BS_2\rangle$ is the overlap integral between the two nonorthogonal broken symmetry Slater determinants. Similarly, the $S_z = 0$ component of the triplet state given by eq 4 may be written as

$$|T'\rangle = \frac{|BS_1\rangle - |BS_2\rangle}{\sqrt{2(1 - \langle BS_1|BS_2\rangle)}} \quad (8)$$

By taking the energy expectation value of the S' and T' states given by eqs 7 and 8, one has

$$E_{S'} = \frac{E_{BS} + \langle BS_1|\hat{H}|BS_2\rangle}{1 + \langle BS_1|BS_2\rangle} \quad (9)$$

and

$$E_{T'} = \frac{E_{BS} - \langle BS_1|\hat{H}|BS_2\rangle}{1 - \langle BS_1|BS_2\rangle} \quad (10)$$

which, after elimination of the unknown $\langle BS_1|\hat{H}|BS_2\rangle$ term, permits one to write

$$J = E_{S'} - E_{T'} = \frac{2(E_{BS} - E_{T'})}{1 + \langle BS_1|BS_2\rangle} \quad (11)$$

If one further assumes that spin polarization of the closed shells can be neglected, it is easy to show that $\langle BS_1|BS_2\rangle \leq |\langle a|b\rangle|^2$ where $\langle a|b\rangle$ is just the overlap integral, S_{ab} , between the two magnetic orbitals of the BS solution and eq 11 reduces to eq 3. In the present case eq 6 can be used to show that $|\langle a|b\rangle|^2$ is simply given by $4\lambda^2\mu^2$, but in a general case it must be exactly computed.

Apart from the relationship between J and the energies of the triplet and broken symmetry states, the above reasoning permits one to obtain the spin density on a given center, ρ_A , as arising from the BS solution. In fact

$$\rho_A = \lambda^2 - \mu^2 \quad (12)$$

from which one obtains

$$\begin{aligned} 2\lambda^2 &= 1 + \rho_A \\ 2\mu^2 &= 1 - \rho_A \end{aligned} \quad (13)$$

and recalling that on the present simple example $|\langle a|b\rangle|^2 = 4\lambda^2\mu^2$ one may relate the spin density on a magnetic center to this overlap matrix in a very simple way

$$|\langle a|b\rangle|^2 = 1 - \rho_A^2 \quad (14)$$

This simple equation permits one to relate the effect of nonorthogonality to the spin density on the magnetic centers. We must point out that given the simplicity of the model used

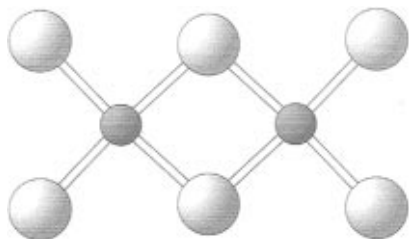


Figure 1. Schematic representation of the planar conformation of $[\text{Cu}_2\text{Cl}_6]^{2-}$ binuclear complex.

to derive this relationship, eq 14 has to be regarded more as a tool of understanding the effect of nonorthogonality than as a way to estimate the overlap integral. We will show that, in some simple cases, eq 14 provides a quite accurate, simple, and alternative way to take into account the nonorthogonality of the spin orbitals entering into the BS solution. However, in realistic systems with polarizable core, the spin polarization of the core may be responsible for a lowering of the $\langle \text{BS}_1 | \text{BS}_2 \rangle$ overlap integral, as well as for the contribution of the core to the atomic spin density ρ_A . Moreover, the ab initio spin density is calculated through the Mulliken approximation. So the use of eqs 11 and 14 is neither equivalent nor completely reliable. For these realistic systems, the effect of nonorthogonality has to be investigated by explicit computation of the $\langle \text{BS}_1 | \text{BS}_2 \rangle$ overlap integral.

III. Computational Details

To check which is the influence of the overlap between magnetic orbitals into the J value resulting from the use of the broken symmetry approach, we present test calculations on three different model systems. The systems chosen in the present work are H–He–H, $[\text{Cu}_2\text{Cl}_6]^{2-}$ and La_2CuO_4 . The first of these examples is included because the full CI solution is available and, hence, it has been sometimes used as a model system.^{37,38} The second system belongs to a broad class of complexes that have long been used as references for experimental magnetostructural correlations³⁹ and, more recently,^{9,10,40} as reference for very accurate ab initio calculations based on the newly developed difference dedicated configuration interaction, DDCI, method.⁹ Finally, our third example corresponds to La_2CuO_4 , one of the superconductor parent compounds for which methods based on the local density approximation fail to properly predict its antiferromagnetic order.⁴¹ This failure may be overcome by making use of more accurate exchange-correlation functionals^{42–46} or by applying ab initio methods to a cluster model representation of the physical compound.^{16,20,21}

For the first system, we have considered three different geometries corresponding to different H–He bond distances. Following Hart et al.³⁸ we use 1.25, 1.625, and 2.00 Å. Similarly, for $[\text{Cu}_2\text{Cl}_6]^{2-}$ we have chosen the planar conformation (Figure 1) for which there is experimental³⁹ and theoretical^{9,10,47} evidence of a weak antiferromagnetic interaction. For comparison purposes bond distances and bond angles for $[\text{Cu}_2\text{Cl}_6]^{2-}$ are the same used by Miralles et al. in their DDCI study. Hence, the Cu–Cl(bridge) distance is 2.30 Å, the Cu–Cl(ligand) 2.26 Å, and the Cu–Cl–Cu and Cl–Cu–Cl angles are 95° and 93°, respectively. Finally, for La_2CuO_4 we use a cluster model representation of the extended systems. This cluster contains two Cu^{2+} cations, the bridge O^{2-} , anion and the 10 anions surrounding this basic unit. The resulting cluster is $[\text{Cu}_2\text{O}_{11}]^{18-}$ where the charge is just to indicate that the number of electrons correspond to that of an ionic situation. However, we must point out that the cluster wave functions or densities are flexible enough so as not to be biased to any

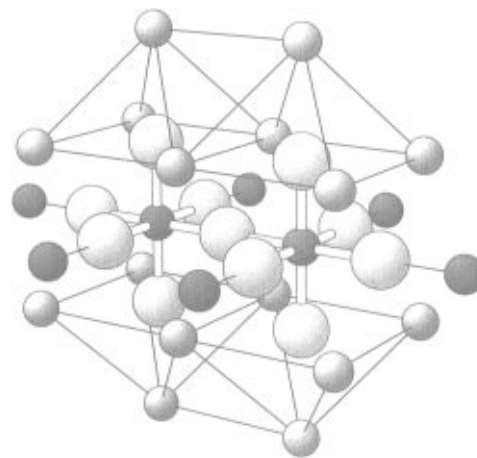


Figure 2. Cu_2O_{11} cluster model used to represent La_2CuO_4 . Also shown are the total ion potentials for the nearest La^{3+} and Cu^{2+} cations surrounding the Cu_2O_{11} cluster. Thick lines link cluster atoms while thin lines link cluster atom to TIPs; small dark spheres represent Cu^{2+} , small light spheres La^{3+} cations, and large spheres O^{2-} anions.

particular description. The Cu_2O_{11} cluster is further embedded in an appropriate environment to represent the rest of the crystal. This environment contains two well-defined different regions. In the first one, total ion potentials^{48,49} (TIPs) are used to represent the La^{3+} cations near to the cluster magnetic centers and, also, to represent the Cu^{2+} cations directly connected to the cluster oxygen anions. These TIPs have a charge of either +2 or +3, depending on whether they represent Cu^{2+} or La^{3+} cations. The second region of the environment consists of an appropriate array of point charges placed at the ion sites and using the parameters derived from the experimental crystal data. A schematic representation of the Cu_2O_{11} cluster model used for La_2CuO_4 is given in Figure 2. The particular point charges employed here are the same used by Martin,¹⁶ and the requirement of the TIPs placed in the first region prevents an artificial polarization of the cluster anion electrons toward the nearest positive point charges.⁵⁰ Further details concerning the number of TIPs and point charges for La_2CuO_4 are described in ref 21. The geometrical parameters were taken from experimental crystal data, i.e., $a = 3.7794$ Å and $c = 13.2260$ Å with the $I4/mmm$ spatial group.

For each one of the different models we have computed the magnetic coupling constant making use of the broken symmetry approach and a variety of spin-polarized methods and rather extended basis sets. For the H–He–H model system the basis set was 6-31++G**, for Cu the 6-3111+g basis set was used for both $[\text{Cu}_2\text{Cl}_6]^{2-}$ and Cu_2O_{11} , the basis set for the Cl and bridge O of the Cu_2O_{11} basis was 6-31G*, and 6-31G was used for the environmental oxygen atoms of this cluster. These methods start from quite opposite extremes. On one hand we have the LDA approximation where the expression suggested by Vosko, Wilk, and Nusair is used.⁵¹ The LDA is believed to produce results that will be representative of the so-called strongly delocalized case. On the other extreme we have the unrestricted Hartree–Fock (UHF) method, which at first glance will lead to the strong localized limit. To include methods that behave somehow between LDA and UHF, we include results from generalized gradient-corrected functionals. In particular, we employ the Becke exchange⁵² with the Perdew–Wang⁵³ correlation functional; this will be denoted by B–PW. We consider some examples of hybrid functionals. In particular we use the exchange Becke three-parameter functional⁵⁴ again with the PW correlation functional and also with the one suggested by Lee et al;⁵⁵ these two approaches will be

TABLE 1: Calculated Values of Spin Density, ρ , and Expectation Value of the Total Square Spin Operator, $\langle\hat{S}_z^2\rangle$, for the $|T\rangle$ and $|BS\rangle$ States of H–He–H at Three Different Distances. Also Given Is the Overlap between the Magnetic Orbitals of the $|BS\rangle$ State

distance	method	$ T\rangle$		$ BS\rangle$		$\langle a b\rangle$
		ρ	$\langle\hat{S}_z^2\rangle$	ρ	$\langle\hat{S}_z^2\rangle$	
1.25	UHF	1.0628	2.001	1.0240	0.945	0.2347
	LDA	1.0464	2.001	0.6920	0.445	0.7447
	B–PW	1.0551	2.001	0.8681	0.696	0.4549
	B3–PW	1.0544	2.001	0.9274	0.793	0.4549
	B3–LYP	1.0497	2.001	0.8996	0.750	0.5004
	HFS–null	1.0564	2.001	0.9774	0.872	0.3573
1.625	UHF	1.0202	2.000	1.0159	0.994	0.0761
	LDA	1.0118	2.000	0.9799	0.940	0.2454
	B–PW	1.0173	2.000	1.0043	0.979	0.1469
	B3–PW	1.0170	2.000	1.0062	0.983	0.1330
	B3–LYP	1.0151	2.000	1.0015	0.976	0.1544
	HFS–null	1.0175	2.000	1.0094	0.987	0.1167
2.000	UHF	1.0068	2.000	1.0062	0.999	0.0247
	LDA	1.0033	2.000	1.0009	0.994	0.0777
	B–PW	1.0066	2.000	1.0058	0.998	0.0403
	B3–PW	1.0063	2.000	1.0054	0.999	0.0385
	B3–LYP	1.0055	2.000	1.0042	0.998	0.0484
	HFS–null	1.0058	2.000	1.0052	0.999	0.0382

abbreviated as B3–PW and B3–LYP, respectively. Finally, following a very recent work by Martin and Illas,⁵⁶ we explore a half-and-half functional that mixes 50% of Slater and Hartree–Fock exchange and does not include any correlation part; this last computational model will be referred to as HFS–null.

All energy calculations have been carried out using the Gaussian-94⁵⁷ suite of programs, while overlap elements have been computed with the aid of some local software coupled to the HONDO-CIPSI package.⁵⁸ Given the small energy differences involved, special care has been taken to control convergence in the self-consistent field procedure and in the numerical integration steps. Results reported in the next section have been found to be stable with respect to these two numerical parameters.

IV. Results and Discussion

To center the discussion, we report in Table 1 results for the H–He–H model system. These include the spin density on the magnetic center, for both $|T\rangle$ and $|BS\rangle$ states, as obtained from each computational method. We also include the expectation value of the total square spin operator, $\langle\hat{S}_z^2\rangle$, which for $|T\rangle$ must be close to 2.000 and for $|BS\rangle$ must approach 1.000, we will see that for some functionals this is not the case. Finally, we report the $\langle a|b\rangle$ values computed from the different sets of molecular, Hartree–Fock or Kohn–Sham, orbitals. These values have been obtained after a proper corresponding orbital transformation aimed to obtain α and β orbitals, which taken as couples resemble as much as possible closed shells. This permits one to approximate the $\langle BS_1|BS_2\rangle$ integral by $|\langle a|b\rangle|^2$. Similarly, Table 2 collects the equivalent results for the two other model systems.

From Tables 1 and 2 we see that there is a general tendency of LDA to produce quite large overlaps. For the La_2CuO_4 model it is really close to the delocalized limit. However, we will show that this cannot be interpreted as a case exhibiting strongly delocalized magnetic orbitals but rather as the failure of LDA to properly describe this system as antiferromagnetic. It reflects one of the largest limitations of LDA, which predicts Mott–Hubbard insulators to behave as metals. Apart from the LDA approach, and to some extent the BPW one, the rest of the DFT

TABLE 2: Calculated Values of Spin Density, ρ , and Expectation Value of the Total Square Spin Operator, $\langle\hat{S}_z^2\rangle$, for the $|T\rangle$ and $|BS\rangle$ States of $[\text{Cu}_2\text{Cl}_6]^{2-}$ and for the Cu_2O_{11} Cluster Model Representation of La_2CuO_4 . Also Given Is the Overlap between the Magnetic Orbitals of the $|BS\rangle$ State

system	method	$ T\rangle$		$ BS\rangle$		$\langle a b\rangle$
		ρ	$\langle\hat{S}_z^2\rangle$	ρ	$\langle\hat{S}_z^2\rangle$	
$[\text{Cu}_2\text{Cl}_6]^{2-}$	UHF	0.8883	2.006	0.8907	1.005	0.0086
	LDA	0.4692	2.001	0.4478	0.872	0.3528
	B–PW	0.4973	2.002	0.4873	0.930	0.2588
	B3–PW	0.5683	2.004	0.5697	0.991	0.2193
	B3–LYP	0.5630	2.004	0.5642	0.991	0.2196
	HFS–null	0.7083	2.006	0.7113	1.004	0.0313
Cu_2O_{11}	UHF	0.9051	2.004	0.8983	1.003	0.0342
	LDA	0.6372	2.001	0.3414	0.295	0.8280
	B–PW	0.6629	2.001	0.5066	0.605	0.6082
	B3–PW	0.7279	2.002	0.6932	0.943	0.2176
	B3–LYP	0.7258	2.002	0.6912	0.943	0.2204
	HFS–null	0.8136	2.004	0.7979	0.991	0.0861

TABLE 3: Calculated Values of $-J$, in cm^{-1} , for the H–He–H System at Three Different Distances and Assuming That the S_{ab} Overlap Integral (cf. Eqs 3 and 11) Is Zero, $\langle a|b\rangle$, Given Approximately by Eq 14, or Taken as Unity

distance	method	$-J$	$-J$	$-J$	$-J$
		($S_{ab} = 0$)	($S_{ab} = \langle a b\rangle$)	($S_{ab} = \text{eq 14}$)	($S_{ab} = 1$)
1.25	UHF	3856.4	3655.1	4053.1	1928.2
	LDA	12528.7	8058.9	8236.2	6264.3
	B–PW	8703.9	6676.4	6983.4	4352.0
	B3–PW	7594.4	6292.4	6662.4	3797.2
	B3–LYP	8392.7	6711.9	7048.4	4196.3
	HFS–null	5940.2	5267.6	5686.3	2970.1
	FCI		4860		
1.625	UHF	424.9	422.5	439.0	212.5
	LDA	1551.2	1463.0	1491.8	775.6
	B–PW	903.0	883.9	910.8	451.5
	B3–PW	831.2	816.7	841.6	415.6
	B3–LYP	994.2	971.0	997.2	497.1
	HFS–null	697.3	687.9	710.7	348.6
	FCI		544		
2.000	UHF	42.3	42.3	42.9	21.2
	LDA	169.4	168.4	169.7	84.7
	B–PW	88.2	88.0	89.2	44.1
	B3–PW	82.9	82.8	83.9	41.5
	B3–LYP	109.4	109.1	110.3	54.7
	HFS–null	74.3	74.2	75.1	37.1
	FCI		50		

methods tend to produce more delocalized orbitals than UHF. However, this tendency is quite small, and the resulting overlap integral seldom becomes larger than 0.2 indicating that the widely accepted tendency of DFT to produce more delocalized orbitals is not fully justified.

Next, let us turn our attention toward the values of the magnetic coupling constant, J , that are obtained from eq 3 considering explicitly the value of the overlap integrals and comparing to the cases where it is taken arbitrarily as zero or one. Also, we consider the accuracy of eq 14, which provides an indirect way to take the nonorthogonality of α and β magnetic orbitals into account. Results for H–He–H are reported in Table 3, whereas those of the two Cu systems are reported in Table 4. Before entering into the discussion concerning the use of the broken symmetry approach to magnetic coupling, we must point out that for both $[\text{Cu}_2\text{Cl}_6]^{2-}$ and Cu_2O_{11} systems, results from the ab initio difference dedicated CI are in rather good agreement with experiment.^{10,21} For La_2CuO_4 the agreement is even better if a nonorthogonal CI technique is used.²³ These ab initio techniques are, of course, free of the problems encountered by the broken symmetry approach.

TABLE 4: Calculated Values of $-J$, in cm^{-1} , for $[\text{Cu}_2\text{Cl}_6]^{2-}$ and for the Cu_2O_{11} Cluster Model Representation of La_2CuO_4 and Assuming That the S_{ab} Overlap Integral (cf. Eqs 3 and 11) Is Zero, $\langle A|B \rangle$, Given Approximately by Eq 14, or Taken as Unity^a

system	method	$-J$ ($S_{ab} = 0$)	$-J$ ($S_{ab} = a b$)	$-J$ ($S_{ab} = \text{eq 14}$)	$-J$ ($S_{ab} = 1$)
$[\text{Cu}_2\text{Cl}_6]^{2-}$	UHF	-45.6	-45.6	-37.8	-22.8
	LDA	464.5	413.1	258.1	232.3
	B-PW	333.9	312.9	189.4	166.9
	B3-PW	84.3	80.4	50.3	42.1
	B3-LYP	91.0	86.8	54.1	45.5
	HFS-null	-32.0	-31.9	-21.4	-16.0
ab initio	DDCI (10)	6.0			
	exptl	0, 40			
Cu_2O_{11}	UHF	304.1	303.8	254.9	152.1
	LDA	6539.8	3879.7	3472.3	3269.8
	B-PW	4774.1	3485.1	2738.5	2387.1
	B3-PW	1871.8	1787.2	1231.9	935.9
	B3-LYP	1883.6	1796.3	1237.4	941.8
	HFS-null	840.9	834.7	616.8	420.5
ab initio	DDCI (21)	787.2			
ab initio	NOCI (23)	967.9			
	exptl	970			

^a Fully ab initio difference dedicated CI (DDCI) results for both systems and nonorthogonal CI for Cu_2O_{11} are included for comparison.

Now, we will discuss the results from Tables 3 and 4 which exhibit a clear general trend. The LDA largely overestimates the value of J even after properly taking into account the nonorthogonality. Inclusion of gradient-corrected functionals improves somehow the behavior, but results are still far from what can be considered qualitative agreement with either experiment or FCI results. A further improvement is found when using hybrid functionals, but for all systems, the calculated values are still twice the experimental or FCI ones. We notice that if a one assumes a strong delocalized limit, the B3-LYP results for all systems nicely reproduce the experimental or FCI results. On the basis of such an assumption, Ruiz et al.³⁶ invoke good agreement between calculated B3-LYP and experimental results. The present analysis clearly shows that there is no evidence for the strong delocalized behavior of B3-LYP. Hence, good agreement between experiment and B3-LYP results reported by Ruiz et al.³⁶ are likely to arise from an error cancellation resulting from the tendency of B3-LYP to overestimate J by a factor of ≈ 2 (cf. the $S_{ab} = \langle a|b \rangle$ column of Tables 3 and 4) and of the assumption of strong delocalization limit. This later assumption leads to J values that are one-half of those arising from the strong localized limit (see eq 11). The two effects cancel out, and good agreement with experiment is achieved. However, we must point out again that the assumption of the strong delocalized limit is not justified. From the results in the tables it is clear that to obtain a rigorous test on the accuracy of a given DFT method one needs to explicitly compute the S_{ab} integral. For the simplest system, H-He-H, quantitative agreement can be obtained by simply using eq 14, which does not need any additional information and can be applied by using standard output on the available codes. However, for the more complex systems eq 14 only adds qualitative understanding.

A final comment concerns the behavior of results obtained using the DFT approach. This behavior may be rationalized by making use of the well-known Hubbard model Hamiltonian. In this approach, second-order perturbation theory leads to $J \approx t^2/U$, which permits one to relate J and the parameters t and U defining the Hubbard Hamiltonian. Then, it follows that the changes in J produced by different exchange-correlation functionals will arise from changes in the effective parameters of

the Hubbard Hamiltonian or, more precisely, in the t/U ratio. Let us consider the two-electron-two-center problem in the framework of the Hubbard Hamiltonian. For this model Hamiltonian, the energy of the UHF determinant defined in eq 5 reduces to

$$E^{\text{UHF}} = 2\lambda^2\mu^2U + 4\lambda\mu t \quad (15)$$

which has its minimum value when

$$\lambda\mu = -(t/U) \quad (16)$$

Then, using eqs 12 and 16 it is easy to show that

$$t/U = \sqrt{(1 - \rho^2)}/2 \quad (17)$$

Now, it is possible to use eq 17 to try to justify the DFT results. From Tables 1 and 2, it may be observed that all DFT treatments reduce this spin density of the broken symmetry solution resulting in a broad range of values depending on the DFT model used. For Cu_2O_{11} , for instance, the data reported in Table 2 lead to t/U ratios that are 0.22 for the UHF treatment, 0.47 for LDA, and 0.30 for the HFS-null approach. Hence, the effect of the exchange correlation potentials may be understood as changing the t/U ratio, i.e., the delocalization/repulsion ratio, in a variable extent, which may be dramatically exaggerated, as in LDA. The possible reliability of the DFT results for determining the magnetic coupling rests on the control of this effective t/U ratio. These arguments may give an interpretation to the relatively good results given by the HFS-null approach. Similar results for a series of perovskites have been recently reported by Martin and Illas.⁵⁶

VI. Conclusions

In this work, the effect of nonorthogonality in the broken symmetry approach to magnetic coupling has been explicitly considered for the first time. On the basis of the results for three different systems, representative of a variety of physical situations, we can conclude that the most often quoted trend concerning the much larger degree of delocalization of magnetic orbitals obtained from DFT, as opposite to Hartree-Fock, is not fully justified. Except for the LDA approach, explicit calculation of the appropriate overlap integral shows that it is not correct to assume the strong delocalization limit. In fact, the calculated overlap integrals rarely exceed 0.2, except again for LDA, and by B-PW although in a lesser extent. A new simple and accurate way to estimate the overlap integral entering into the calculation has been proposed and tested. This new procedure only needs the spin density on the magnetic center for the broken symmetry state, a rather standard output in most commonly used quantum chemical codes.

Finally, we would like to briefly comment the consequences of the present work for cases concerning more than one electron per magnetic center. Let us consider the simplest case of two atoms A and B, each of them bearing two unpaired electrons in two equivalent orbitals. Again, one may obtain the UHF solution for the high-spin state

$$|Q\rangle = |\dots i_A i'_A j'_B j_B\rangle \quad (18)$$

having energy E_Q . Except for the spin polarization of the core, this state is a pure quintet, hereafter denoted by $|Q\rangle$. Moreover, two degenerate UHF symmetry broken solutions with $S_Z = 0$ can be obtained. These broken symmetry solutions have energy E_{BS} and can be written as

$$\begin{aligned}
 |\text{BS}_1\rangle &= |\dots aa'\overline{bb'}\rangle \\
 |\text{BS}_2\rangle &= |\dots \overline{aa'}bb'\rangle
 \end{aligned}
 \quad (19)$$

where orbitals a and b are linear combinations of i_A and j_B , respectively, and a' and b' equivalent linear combinations of i'_A and j'_B (cf. eq 6).

The $|\text{BS}_1\rangle$ determinant is close to $T_A^+ T_B^-$, the product of two local triplets on atoms A and B. Here T_A^+ denotes a local triplet on atom A with $S_{zA} = 1$ and T_B^- a local triplet on atom B with $S_{zB} = -1$. Therefore, the low lying triplet state would be

$$|\text{T}\rangle = \frac{|\text{BS}_1\rangle - |\text{BS}_2\rangle}{\sqrt{2(1 - \langle \text{BS}_1 | \text{BS}_2 \rangle)}} \quad (20)$$

and its energy expectation value

$$E_T = \frac{E_{\text{BS}} - \langle \text{BS}_1 | \hat{H} | \text{BS}_2 \rangle}{1 - \langle \text{BS}_1 | \text{BS}_2 \rangle} \quad (21)$$

If both $\langle \text{BS}_1 | \text{BS}_2 \rangle$ and $\langle \text{BS}_1 | \hat{H} | \text{BS}_2 \rangle$ (which should be small albeit nonzero!) are simultaneously neglected, it follows that

$$E_Q - E_{\text{BS}} = -2J \quad (22)$$

a result that appears to be identical with that obtained from the use of the Ising model Hamiltonian,²² provided that spin contamination inherent to the UHF approach can be neglected. In fact, from the Ising Hamiltonian it also follows that

$$E_Q - E_T = -2J \quad (23)$$

which already assumes localized magnetic moments. The fact that the broken symmetry approach (cf. eq 22) and the Ising model Hamiltonian (cf. eq 23) lead to the same relationship (again if spin contamination can be neglected!) is because, in this particular case, there is an S_z -eigenfunction, with $S_z = 0$, which appears to be also eigenfunction of the \hat{S}_z spin operator, with total $S = 1$. This particular triplet state is an eigenfunction of both Ising and Heisenberg Hamiltonians. This is the reason eqs 22 and 23 are identical. A similar approach has permitted J to be extracted in recent solid-state calculations.^{59,60}

However, contrary to the one electron per center case described above, if $\langle \text{BS}_1 | \text{BS}_2 \rangle$ and $\langle \text{BS}_1 | \hat{H} | \text{BS}_2 \rangle$ are not neglected, it is impossible to evaluate the $\langle \text{BS}_1 | \hat{H} | \text{BS}_2 \rangle$ quantity from the use of the energy expectation value expression for $|Q(S_z = 0)\rangle$, the $S_z = 0$ component of the high-spin state. In fact,

$$|Q(S_z = 0)\rangle = \frac{1}{\sqrt{6}} |T_A^+ T_B^- + T_A^- T_B^+ + 2T_A^0 T_B^0\rangle \quad (24)$$

where T_A^0 and T_B^0 represent the $S_z = 0$ component of local triplet states on A and B, respectively. The energy associated with $T_A^0 T_B^0$, which is intrinsically multideterminantal, cannot be approached by a UHF calculation. In this case the UHF solution does not provide enough information for a proper, rigorous, evaluation of the triplet state energy and, hence, of the magnetic coupling constant.

Acknowledgment. The authors are indebted to the Spanish "Ministerio de Educación y Cultura" for financial support under CICYT projects PB95-0847-CO2-01 and PB95-0847-CO2-02. I. de P.R.M. is grateful to the University of Barcelona for a predoctoral grant and R.C., O.C., and J.P.M. thank the support

of the European Commission through the TMR network contract ERB FMRX-CT96-0079. The authors also thank the Fundació Catalana de la Recerca and the "Centre de Computació i Comunicacions de Catalunya", C4 CESCA/CEPBA for helping in part of the calculations. Finally we thank Dr. Eliseo Ruiz for helpful discussions concerning nonorthogonality in the broken symmetry approach.

References and Notes

- (1) Heisenberg, W. *Z. Phys.* **1928**, *49*, 619.
- (2) Dirac, P. A. M. *The Principles of Quantum Mechanics*, 3rd. ed.; Clarendon: Oxford, 1947; Chapter IX.
- (3) Herring, C. *Magnetism*; Rado, G. T., Suhl, H., Eds.; Academic Press: New York, 1965; Vol. 2B.
- (4) Nesbet, R. K. *Ann. Phys.* **1958**, *4*, 87; *Phys. Rev.* **1960**, *119* 658; *Phys. Rev.* **1961**, *122*, 1497.
- (5) Anderson, P. W. *Phys. Rev.* **1959**, *115*, 5745; *Solid State Phys.* **1963**, *14*, 99.
- (6) Maynau, D.; Durand, Ph.; Daudey J. P.; Malrieu, J. P. *Phys. Rev. A* **1983**, *28*, 3193.
- (7) de Loth, Ph.; Cassoux, P.; Daudey, J. P.; Malrieu, J. P. *J. Am. Chem. Soc.* **1981**, *103*, 4007.
- (8) Daudey, J. P.; de Loth, Ph.; Malrieu, J. P. in *Magnetic Structural Correlation in Exchange Coupled Systems*, NATO Symposium; Gatteschi, D., Kahn, O., Willett, R. D.; Eds.; Reidel: Dordrecht, 1984.
- (9) Miralles, J.; Castell, O.; Caballol, R. *Chem. Phys.* **1994**, *179*, 377.
- (10) Miralles, J.; Daudey, J. P.; Caballol, R. *Chem. Phys. Lett.* **1992**, *198*, 555. Miralles, J.; Castell, O.; Caballol, R.; Malrieu, J. P. *Chem. Phys.* **1993**, *172*, 33.
- (11) Castell, O.; Caballol, R.; Subra, R.; Grand, A. *J. Phys. Chem.* **1995**, *99*, 154.
- (12) Handrick, K.; Malrieu, J. P.; Castell, O. *J. Chem. Phys.* **1994**, *3*, 101.
- (13) Castell, O.; Caballol, R.; Garcia, V. M.; Handrick, K. *Inorg. Chem.* **1996**, *35*, 1609.
- (14) Wang, C.; Fink, K.; Staemmler, V. *Chem. Phys.* **1995**, *192*, 25.
- (15) Illas, F.; Casanovas, J.; Garcia-Bach, M. A.; Caballol, R.; Castell, O. *Phys. Rev. Lett.* **1993**, *71*, 3549.
- (16) Martin, R. L. *J. Chem. Phys.* **1993**, *98*, 8691.
- (17) Casanovas, J.; Illas, F. *J. Chem. Phys.* **1994**, *100*, 8257.
- (18) Casanovas, J.; Illas, F. *J. Chem. Phys.* **1994**, *101*, 7683.
- (19) Casanovas, J.; Rubio, J.; Illas, F. In *New Challenges in Computational Quantum Chemistry*; Broer, R., Aerts, P. J. C., Bagus, P. S., Eds.; Department of Chemical Physics and Material Science Centre, University of Groningen: Groningen, 1994; pp 214–226.
- (20) Van Oosten, A. B.; Broer, R.; Nieuwpoort, W. C. *Int. J. Quantum Chem. Symp.* **1995**, *29*, 241.
- (21) Casanovas, J.; Rubio, J.; Illas, F. *Phys. Rev. B* **1996**, *53*, 945.
- (22) Moreira, I. de P. R.; Illas, F. *Phys. Rev. B* **1997**, *55*, 4129.
- (23) Van Oosten, A. B.; Broer, R.; Nieuwpoort, W. C. *Chem. Phys. Lett.* **1996**, *257*, 207.
- (24) de Graaf, C.; Illas, F.; Broer, R.; Nieuwpoort, W. C. *J. Chem. Phys.* **1997**, *106*, 3287.
- (25) Norman, J.G., Jr.; Ryan, P. B.; Noodleman, L. *J. Am. Chem. Soc.* **1980**, *102*, 4279.
- (26) Noodleman, L. *J. Chem. Phys.* **1981**, *74*, 5737.
- (27) Noodleman, L.; Baerends, E. J. *J. Am. Chem. Soc.* **1984**, *106*, 2316.
- (28) Noodleman, L.; Norman Jr., J.G.; Osborne, J. H.; Aizman, A.; Case, D. A. *J. Am. Chem. Soc.* **1985**, *107*, 3418.
- (29) Muesca, J. M.; Noodleman, L.; Case, D. A.; Lamotte, B. *Inorg. Chem.* **1995**, *34*, 4347.
- (30) Muesca, J. M.; Noodleman, L.; Case, D. A. *Int. J. Quantum Chem.: Quantum Biol. Symp.* **1995**, *22*, 95.
- (31) Noodleman, L.; Davidson, E. R. *Chem. Phys.* **1986**, *109*, 131.
- (32) Noodleman, L.; Case, D. A. *Adv. Inorg. Chem.* **1992**, *38*, 423.
- (33) Ross, P. K.; Solomon, E. I. *J. Am. Chem. Soc.* **1991**, *113*, 3246.
- (34) Averill, B. A.; Herskovitz, T.; Holm, R. H.; Ibers, J. A. *J. Am. Chem. Soc.* **1973**, *95*, 3523.
- (35) Bencini, A.; Gatteschi, D. *J. Am. Chem. Soc.* **1986**, *108*, 5763.
- (36) Ruiz, E.; Alemany, P.; Alvarez, S.; Cano, J. *J. Am. Chem. Soc.* **1997**, *119*, 1297.
- (37) Bencini, A.; Totti, F.; Daul, C.; Doclo, K.; Fantucci, P.; Barone, V., preprint.
- (38) Hart, J. R.; Rappé, A. K.; Gorun, S. M.; Upton, T. H. *J. Phys. Chem.* **1992**, *96*, 6264.
- (39) Willet, R. D. In *Magneto Structural Correlations in Exchange Coupled Systems*; Willet, R. D., Gatteschi, D., Kahn, O., Eds.; NATO Advanced Studies Series C; Reidel: Dordrecht, 1985; p 140.
- (40) Castell, O.; Caballol, R.; Miralles, J. *Chem. Phys.* **1994**, *179*, 377.
- (41) Pickett, W. E. *Rev. Mod. Phys.* **1989**, *61*, 433.
- (42) Svane, A. *Phys. Rev. Lett.* **1992**, *68*, 1900.

- (43) Svane, A.; Gunnarsson, O. *Phys. Rev. Lett.* **1990**, *65*, 1148.
- (44) Czyzyk, M. T.; Sawatzky, G. A. *Phys. Rev. B* **1994**, *49*, 14211.
- (45) Anisimov, V. I.; Korotin, M. A.; Zaanen, J. A.; Andersen, O. K. *Phys. Rev. Lett.* **1992**, *68*, 345.
- (46) Wei, P.; Qi, Z. Q. *Phys. Rev. B* **1994**, *49*, 12519.
- (47) Broer, R.; Maaskant, W. J. A. *Chem. Phys.* **1986**, *102*, 103.
- (48) Winter, N. W.; Pitzer, R. M. *J. Chem. Phys.* **1988**, *89*, 446.
- (49) Fernández-García, M.; Conesa, J. C.; Illas, F. *Surf. Sci.* **1996**, *349*, 207.
- (50) Sousa, C.; Illas, F.; Pacchioni, G. *J. Chem. Phys.* **1993**, *99*, 6819.
- (51) Vosko, S. H.; Wilk, L.; Nusair, M. *Can J. Phys.* **1980**, *58*, 1200.
- (52) Becke, A. D. *Phys. Rev. A* **1988**, *38*, 3098.
- (53) Perdew, J. P.; Wang, Y. *Phys. Rev. B* **1986**, *33*, 8800. Perdew, J. P.; Wang, Y. *Phys. Rev. B* **1992**, *45*, 13244.
- (54) Becke, A. D. *J. Chem. Phys.* **1993**, *98*, 5648.
- (55) Lee, C.; Yang, W.; Parr, R. G. *Phys. Rev. B* **1988**, *37*, 785.
- (56) Martin, R. L.; Illas, F., preprint.
- (57) Frisch, M. J.; Trucks, G. W.; Schlegel, H. B.; Gill, B. G.; Johnson, P. M. W.; Robb, M. A.; Cheeseman, J. R.; Keith, T.; Petersson, G. A.; Montgomery, J. A.; Raghavachari, K.; Al-Laham, M. A.; Zakrzewski, V. G.; Ortiz, J. V.; Foresman, J. B.; Peng, C. Y.; Ayala, P. Y.; Chen, W.; Wong, M. W.; Andres, J. L.; Replogle, E. S.; Gomperts, R.; Martin, R. L.; Fox, D. J.; Binkley, J. S.; Defrees, D. J.; Baker, J.; Stewart, J. P.; Head-Gordon, M.; Gonzalez, C.; Pople, J. A. *Gaussian 94*, Revision B.4; Gaussian, Inc.: Pittsburgh, PA, 1995.
- (58) Dupuis, M.; Rys, J.; King, H. F. HONDO-76, program 338, QCPE, University of Indiana, Bloomington, IN 47401. HONDO-CIPSI-DDCI package written by R. Caballol, O. Castell, J. P. Daudey, S. Evangelisti, F. Illas, J. P. Malrieu, D. Maynau, M. Pelissier, J. Rubio, and F. Spiegelmann.
- (59) Ricart, J. M.; Dovesi, R.; Roetti, C.; Saunders, V. R. *Phys. Rev. B* **1995**, *52*, 2381.
- (60) Dovesi, R.; Ricart, J. M.; Saunders, V. R.; Orlando, R. *J. Phys. Condens. Matter* **1995**, *7*, 7997.